Malaysian Journal of Computing, 9 (2): 1955-1978, 2024 Copyright ©
UiTM Press
eISSN: 2600-8238

PREDICTING COVID-19 TRENDS: A DEEP DIVE INTO TIME-DEPENDENT SIRSD WITH DEEP-LEARNING TECHNIQUE

Abdul Basit[1*], Jasni Mohamad Zain[2], Abdul Kadir Jumaat[3], Nur'Izzati Hamdan[4] and Hafiza Zoya Mojahid[5]

[1,2,3,4,5]College of Computing, Informatics and Mathematics, Universiti Teknologi Mara, Shah Alam, Selangor, Malaysia*
[2,3]Institute for Big Data Analytics and Artificial Intelligence(IBDAAI), Kompleks Al-Khawarizmi, Universiti Teknologi Mara, Shah Alam, Selangor, Malaysia

[1*]2021691374@student.uitm.edu.my, [2]jasni67@uitm.edu.my,
[3]abdulkadir@tmsk.uitm.edu.my,
[4]nurizzati@tmsk.uitm.edu.my,
[5]2022547787@student.uitm.edu.my

ABSTRACT

The COVID-19 pandemic, also known as Coronavirus Disease 2019, has affected over 700 million people globally, resulting in approximately 7 million deaths. Research has proposed multiple mathematical models to institute a disease transmission framework and predict the disease growth. Most of the existing mathematical disease growth prediction models are less effective due to the exclusion of the re-susceptible scenarios and overlooks their time-dependent properties, which change continuously during the viral transmission process. Another popular prediction technique is deep learning approaches. However, existing methods often fail to accurately capture the dynamic trends of epidemics during their spreading phases in short-term and medium term. Therefore, inspired by the deep learning approach, this study offers a new model for COVID-19 prediction centered on time-dependent namely Susceptible-Infected-Recovered-re-Susceptible-Death-Deep Learning (SIRSD-DL) model. This model proposes a combination of deep learning techniques, specifically Feed-Forward Neural Networks (FFNN) and Recurrent Neural Networks (RNN), with an epidemiological mathematical framework. It aims to forecast the parameters of SIRSD model by incorporating deep learning technology With the current COVID-19, we examined data from seven countries—China, Malaysia, India, Pakistan, South Korea, the United Arab Emirates and the United States of America—between March 15, 2020, till May 27, 2021. Our research demonstrates that the proposed model outperforms both standalone and hybrid techniques, offering enhanced predictability for short- and medium-term forecasts. In India, the model achieved prediction accuracies by Mean Absolute Percentage Error of 0.82% for 1-day, 1.48% for 3-day, 2.72% for 7-day, 2.50% for 14-day, 3.73% for 21-day, and 6.63% for 28-day forecasts. This approach is expected to be valuable not only for COVID-19 but also for forecasting future pandemics.

Keywords*: Mathematical Model, Deep Learning, FFNN, RNN, SIRSD, Prediction*.

Received for review: 09-09-2024; Accepted: 27-09-2024; Published: 01-10-2024
DOI: 10.24191/mjoc.v9i2.27425

1. Introduction

Severe-Acute-Respiratory-Syndrome-Coronavirus-2 (SARS-CoV-2), a new kind of coronavirus, was first identified in Wuhan, Hubei Province, China in late December 2019. This virus causes a highly infectious sickness termed COVID-19, which has spread globally. On March 12, 2020, the World Health Organization (WHO) declared a pandemic. SARS-CoV-2 is primarily spread among people via infected surfaces and respiratory droplets from coughing, sneezing, and talking (Hu *et al*., 2020). The most notable feature of SARS-CoV-2 is its ability to spread rapidly, as it can survive on various surfaces for hours to nine days at ambient temperature (Chu *et al*., 2022). This virus can induce multiple organ failure or Acute Respiratory Distress Syndrome (ARDS), which can worsen an infected individual's physiological state and even result in death (Van Doremalen *et al*., 2020).

Three fundamental methods exist for forecasting the dynamics of an epidemic: learning-based techniques (Machine Learning (ML) and Deep Learning (DL)), statistical techniques, and mathematical models (Zeroual *et al*., 2020). A common example is the Susceptible-Infected-Removed (SIR) model, widely used to simulate the spread of infectious disease. It uses the nonlinear equations to divide a population into mutually exclusive groups, representing the evolution of each category (Tang *et al*., 2020). To develop compartmental models that describe the progression of an epidemic, statistical approaches extract general statistics from the data (Zhang *et al*., 2022). Another well-known approach is the Susceptible-Exposed-Infected-Recovered (SEIR) model. Many studies have focused on modifying and refining these foundational models to enhance predictive accuracy and applicability.

The essential contamination number and exponential progression rate can be dynamically measured using the time frame method for variant data analysis, which forms the basis of the generalized adaptive SIR prediction model proposed by Liao *et al*. (2020) presented. Singh and Gupta (2022) introduced the Generalized-SIR (G-SIR) model, which incorporates multi-day reported cases. According to experimental evaluations conducted on data from several countries, this model is capable of providing real-time probability estimates and monitoring the progression of the COVID-19 outbreak. Cooper *et al*. (2020) proposed a hypothetical framework for investigating the communal spread of COVID-19, where the number of susceptible individuals was treated as a variable within the mathematical SIR model. Caputo derivatives were utilized by Mohammadi *et al*. (2022) to develop a Susceptible-Infected-Recovered-Deceased (SIRD) model based on fractional-order calculus for disease spread. The second surge of the pandemic in Japan and Iran was forecasted using mathematical modeling with different order derivatives.

Ramezani *et al*. (2021) introduced a modified Susceptible-Exposed-Infected-Recovered-Death (SEIRD) approach to account for asymptomatic infections and to capture the non-linear dynamics of the global disease. According to Holmdahl and Buckee (2020), mathematical simulations of transmissible diseases are valuable for assessing epidemic spread; however, the accuracy of these models is constrained by the assumptions made in defining input parameters. The uncertainty of the model increases when unknown parameters must be estimated through model fitting. Moreover, the variability of model parameters is influenced by a range of factors, making it challenging for a single model to capture the complexity of real-world conditions. To achieve accurate predictions of COVID-19 dynamics, more advanced techniques that account for multiple aspects of the virus transmission pathway are necessary (Panovska-Griffiths, 2020).

Machine learning (ML) algorithms are employed in ML-based approaches to evaluate past data and identify trends that provide precise estimates of the number of new infections (Aimran *et al*., 2022). Any method used to make judgments with significant consequences should, presumably, be both accurate and comprehensible; it should provide the administration with sufficient data to support its recommendations (Rudin, 2019). Deep learning is a relatively recent approach that has been increasingly applied in the research and forecasting of the COVID-19 disease. Nabi *et al*. (2021) evaluated four deep learning models: Convolutional Neural Networks (CNN), Gated Recurrent Units (GRU), Multivariate Convolutional Neural Networks (MCNN), and LSTM networks. Their analysis demonstrated that CNN outperformed the other deep learning frameworks in terms of prediction consistency and

accuracy, establishing it as the most reliable model among those assessed.

Devaraj *et al.* (2021) analyzed and forecasted the global cumulative counts of infection, recovery, and death cases using Prophet models, LSTM networks, Stacked LSTM networks, and ARIMA models. Their results indicated that the Stacked LSTM model provided the most precise predictions, achieving an error margin of less than 2%, surpassing the other methods evaluated. The fundamental approach of integrating deep learning with compartmental models involves replacing the fixed variables in traditional models with time-dependent coefficients that can be identified through dataset analysis (Liao *et al*., 2020; Anastassopoulou *et al*., 2020; Chen *et al*., 2020). Most methods, however, do not predict the number of new infections; instead, they focus on identifying the factors that might explain historical data. It is important to note that while these methods can provide insights into the nuances of the disease, there is no guarantee that those parameters can accurately forecast future behavior.

Liao *et al.* (2021) developed a hybrid forecasting framework based on a time-varying Susceptible-Infected-Recovered-Vaccined-Death-Deep Learning (SIRVD-DL) model utilizing deep learning techniques such as GRU, Vanilla LSTM, Stacked LSTM and Bidirectional LSTM. Compared to traditional deep learning approaches, this model achieved a 50% enhancement in single-day forecasting accuracy. Moreover, it may be modified to make short-term and medium-term forecasts, thereby enhancing the overall accuracy and reliability of the outcomes. These findings suggest that deep learning methodologies can yield accurate one-day predictions for COVID-19 cases.

However, these standalone and hybrid approaches face three significant limitations. First, existing methods often fail to accurately capture the dynamic trends of epidemics during their spreading phases in short-term and medium term, as they predominantly rely on numerical fitting techniques. Second, there is minimal variability in the number of infected individuals over time, which further limits the effectiveness of these approaches. Third, hybrid approaches often involve high complexity, which increases computational demands and diminishes interpretability. For the development of healthcare policies and strategic plans, models that offer improved short-term and medium-term predictions are highly valuable. Integrating deep learning techniques with epidemiological models in a non-complex manner can enhance predictive accuracy while maintaining interpretability. Such integration provides vital insights into the expansion of infectious diseases, thereby supporting more informed decision-making and policy formulation. Consequently, adopting streamlined, interpretable models is essential for effective epidemic management and planning.

In this paper, we mainly contribute the following: (1) Enhancing the interpretability of prediction algorithms through the integration of time-varying and re-susceptible cases in a new mathematical model, namely Susceptible-Infected-Recovered-re-Susceptible (SIRSD). (2) This approach introduces an advanced version of the traditional SIRD model by incorporating an additional re-susceptible compartment, which enables the evaluation of variable parameters and improves the models adaptability to real-world dynamics. (3) Furthermore, we propose a new hybrid deep learning algorithm that integrates the strengths of a Feed-Forward Neural Network (FFNN) and a Recurrent Neural Network (RNN) for parameter prediction. This hybrid framework processes parameters determined via a least squares approach to accurately forecast critical variables influencing the spread of COVID-19. (4) The predicted parameters are then reintegrated into the new SIRSD framework, defining our proposed model, namely the Susceptible-Infected-Recovered-re-Susceptible-Death-Deep Learning (SIRSD-DL), resulting in precise estimations of infection numbers and providing valuable insights for public health interventions. Following significant computations, we focus on answering three major research questions.

- RQ1: Does the effectiveness and efficiency of the time-varying least-squares algorithm align with its underlying logic?
- RQ2: What is the prediction performance of the SIRSD-DL algorithm? How much better is it than standalone deep learning techniques? What is the algorithms efficacy for short- and medium-term predictions?

- RQ3: How well does the presented hybrid FFNN-RNN technique work for determining the parameters when combined with feature selection? What distinguishes employing this procedure from not applying it?

The structure of this research paper is as follows: The first section begins with the Introduction. The second section introduces the Susceptible-Infected-Recovered-re-Susceptible-Death-Deep Learning (SIRSD-DL) predicting framework, while the third section demonstrates the proposed models effectiveness through computational experiments, statistical analysis, and comparisons with existing literature. Finally, the conclusion section summarizes the key insights and main ideas of the study.

2. Method

The SIRSD-DL prediction model comprises three main stages. The first stage begins with acquiring datasets from two authentic sources: Johns Hopkins University and Our World in Data. This is followed by data preprocessing and calculating parameters by the least squares method for the development of the SIRSD model. The second stage involves the establishment of a hybrid deep learning technique that combines a Feed-Forward Neural Network (FFNN) and a Recurrent Neural Network (RNN) based on feature selection methods to predict parameters such as the rate of infection (beta) and the rate of death (delta). In this stage, the datasets are split into 70% for training and 30% for testing. In the third stage, the projected parameters are then integrated into the SIRSD model to produce predictions of infected cases as well as other trends. The primary objective of the SIRSD-DL model is to assess the variations in infection characteristics to construct an optimal simulation for predicting the outbreak trajectory. Figure 1 depicts a summary of the research methodology.

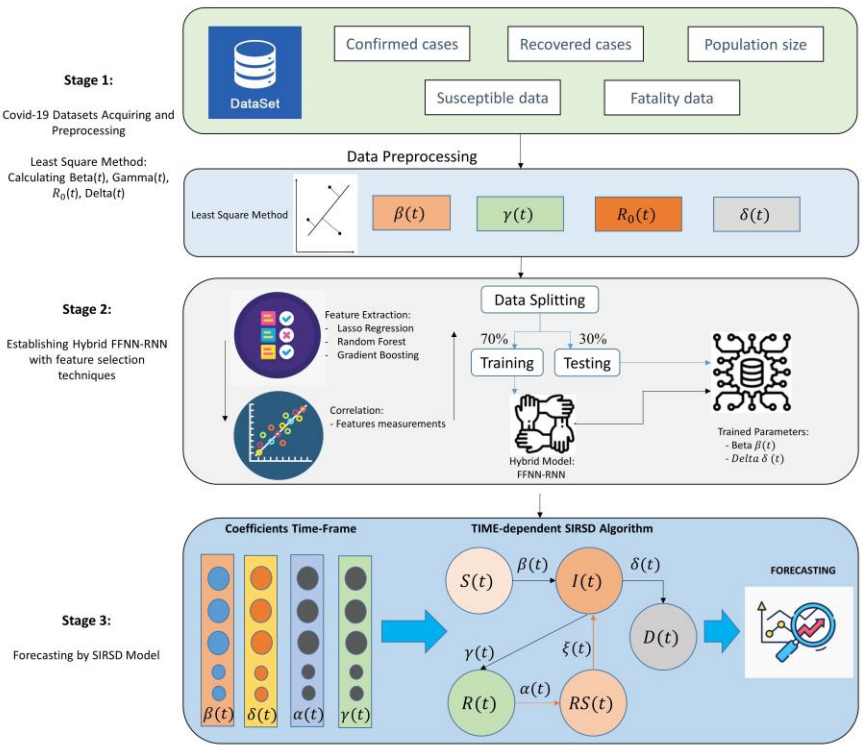

Figure 1. The operational structure of the SIRSD-DL forecasting model.

The remainder of this section provides a detailed description of the contents and methodology of each part.

2.1 Datasets and Features

Since the onset of the COVID-19 pandemic, many nations have released statistics gathered by relevant authorities, including hospitals, clinics, and health agencies, providing real-time observational data for comprehensive analysis and forecasting. This paper utilizes data from two prominent databases. The first source is the Johns Hopkins University Center for Systems Science and Engineering (JHU-CSSE), which provides time-series data on global confirmed infections, recoveries, and fatalities. This dataset, widely used by researchers, offers variables that track the number of cases on specific dates. Table 1 presents a summary of key statistics for infected cases worldwide.

Table 1. Data samples comprising confirmed worldwide cases sourced from Johns Hopkins University.

Province/State	Country/Region	Latitude	Longitude	1/22/20	7/30/21
Hubei	China	30.9756	112.2707	444	68195
Hunan	China	27.6104	111.7088	4	1079
Shandong	China	36.3427	118.1498	2	885
Shanghai	China	31.202	121.4491	9	2307
Hubei	China	30.9756	112.2707	444	68195

Table 2. Sample data on features from Our World in Data.

Location	Iso_code	Date	new_cases_per_million	total_tests	positive_rate
India	IND	2021-05-24	156.872	330536064	0.1219
India	IND	2021-05-25	138.605	332594176	0.1162
India	IND	2021-05-26	147.421	334811496	0.11
India	IND	2021-05-27	149.098	336969353	0.1043

The second dataset is sourced from the Our World in Data platform, which provides comprehensive information on features based upon confirmed COVID-19 cases, hospitalizations, deaths, testing, and other factors affecting infection and mortality rates. The data team at Our World in Data supplied the COVID-19 features used in this study. Table 2 shows sample data for key features such as: 'date' (the observation date), 'hospital patients' (number of hospital admissions), 'location' (geographical region), 'iso_code' (country code), 'total tests' (total tests conducted), and 'positive rate' (percentage of positive tests). Both datasets are integrated to support the hybrid FFNN-RNN technique for predicting the vital parameters like the rate of infection (beta) and the rate of death (delta). While the data is focused on COVID-19, the models structure is adaptable and could be applied to future pandemics, provided similar data is available, thus enhancing its long-term relevance.

2.2 Calculating epidemiological parameters by Least Square Method

The epidemiological model consists of a series of equations that describe the dynamics of how an infectious disease spreads within a susceptible population. Thus, a group of differential equations that can be classified as Susceptible (individuals vulnerable to infection), Infected (individuals with infection) and Recovered (individuals cured from the disease) of time as t. The following equations (1), (2) and (3) are expressed as:

$$\frac{dS}{dt} = -\frac{\beta}{N} SI \tag{1}$$

$$\frac{dI}{dt} = \frac{\beta}{N} SI - \gamma I \tag{2}$$

$$\frac{dR}{dt} = \gamma I \tag{3}$$

In this case, the actual infection rate is represented by β, and the recovery rate by γ. To be more precise, γ can be defined as the reciprocal of the time it takes to recover (γ = 1/d). When there is no spread of infection or I + R = 0 and S≅N. Equation (2) is used to generate the following Equation (4):

$$\frac{dI}{dt} \sim I(\beta - \gamma) \tag{4}$$

After integrating Equation (4), the achieved following Equation (5):

$$I = I_0 e^{(\beta-\gamma)t} \tag{5}$$

During the initiation of infection spread, the count of infectious individuals, I(t), experiences an initial exponential increase as Equation (6).

$$\frac{dI}{dt} \sim zI \tag{6}$$

If we suppose the difference between transmission of infection and recovery rate (β-γ=z), we obtain Equation (7):

$$I(t) = I_0 e^{zt} \tag{7}$$

We apply the natural logarithm on both sides of the equation, we will derive Equation (8):

$$\ln I = zt + \ln I_0 \tag{8}$$

Now, we can estimate the value of *z* using the Covid-19 dataset variables followed by estimating β and γ. To achieve the optimal linear fit, methods such as the least squares approach can be employed. As to compute the parameter recovery rate gamma (γ). Assuming that *I* is constant as I(t)= I_0 that no more infection is taking place in the community, we obtain the Equation (9):

$$\frac{dR}{dt} = \gamma I_0 \tag{9}$$

If the recovery time is denoted as t = t days, and if R(t)=I_0 *or* γt=1, the subsequent equation (9), we get this Equation (10):

$$R(t) = \gamma . t\, I_0 \tag{10}$$

Suppose, if t=A period to recovery, then, R(A)=I_0, hence, the following achieved Equation (11), where t is the recovery period:

$$\gamma \approx \frac{1}{T} \tag{11}$$

Equation (3) is used to get the resultant equation when there is a temporal change of time as $dt=f$. In order to compute the value of γ by computing the average value of the rate of

change of the recovery group such that the product of γ in the infected class is equal to rate of change of removed class in particular time interval, this is how the rate of change is expressed:

$$\gamma I(t) = \frac{R(t+f) - R(t)}{I(t)} \tag{12}$$

The basic reproduction number, defined as R_0 measures the mean frequency of people contaminated by a single host. A higher R_0 value indicates a higher potential for the disease to spread, meaning each infected individual is likely to infect more people, leading to a faster and more widespread outbreak. Mathematically, it is the ratio of the transmission rate to the recovery rate, as shown in Equation (13):

$$R_0 = \frac{\beta}{\gamma} \tag{13}$$

Due to the dynamic nature of COVID-19, the iterative approach involves executing the Least Squares Method algorithm by grouping data over various time spans (e.g., 3 days or 5 days). This allows for the calculation of average parameters (β, γ, R_0) over these grouped periods, providing a more comprehensive dataset for training and testing. By manually executing these iterations across different groupings, we were able to thoroughly examine the derived parameters for each country dataset, ensuring their relevance and accuracy. The number of iterations performed was dependent on the length of the dataset and the analysis of the acquired observations.

Table 3. Least Square Methods Iterations.

No.	Country	Iterations
1	China	31
2	India	42
3	Malaysia	31
4	Pakistan	31
5	South Korea	25
6	UAE	31
7	USA	28

Table 3 lists the number of iterations performed to calculate the vital parameters, which were used to prepare a dataset for the deep learning mechanism. This dataset was then used to predict the parameters that best fit the actual dataset by comparing the predicted and actual infected cases.

2.3 Deep learning-based forecasting technique

The proposed hybrid deep learning technique, which combines FFNN and RNN, is used to predict and evaluate key parameters (β and δ). These predicted parameters are then integrated into the time-series SIRSD model for further analysis and forecasting. The time-series curve representing the number of infected individuals exhibits irregular patterns, making it difficult to establish a consistent sequential trend (Nabi *et al*., 2021). To address this problem, our method first calculates the parameters, revealing the outbreaks cognitive trajectory. Deep learning techniques are employed as they have proven effective in predicting time series data. To enhance the model, feature selection techniques such as LASSO, Random Forest, and Gradient Descent are utilized to identify the most influential features affecting the predicted parameters. Based on the projected parameter values, it then develops the time-dependent SIRSD approach. The forthcoming section will examine the specifics of the proposed hybrid FFNN-RNN method, emphasizing the parameter estimation process supported by feature selection and the assessment metrics used to evaluate the approach.

The significance of this hybrid deep learning approach lies in its ability to enhance

the accuracy and reliability of epidemic forecasting. By integrating FFNN and RNN, we leverage the strengths of both architectures: FFNN for capturing complex relationships in static data and RNN for modeling temporal dependencies in time series. The application of feature selection techniques ensures that only the most relevant variables influence the predictions, reducing noise and improving model interpretability. This targeted approach not only refines parameter estimation but also allows public health officials to make informed decisions based on robust, data-driven insights. Ultimately, by accurately modeling the dynamics of COVID-19 spread, our method contributes to more effective strategies for outbreak management and control.

2.3.1 Feed-Forward Neural Network (FFNN)

Artificial neural networks (ANNs) that are fed forward are currently being used with great success in a variety of applications. One of their main advantages over conventional coding is that they may function without a determined by users algorithm for addressing problems. Like human learning, these neural networks acquire knowledge through examples that are given to them. The inherent generalization capacity of feedforward artificial neural networks (ANNs) is a second important benefit. This suggests that they are able to identify and adjust to variations that resemble but differ from the initial ones they were trained on (Benardos & Vosniakos, 2007). According to the connections regarding neurons, two main network topologies are identified: Feed-Forward Neural Networks (FFNN) as well as Recurrent Neural Networks (RNN). A network that lack feedback coming from neuron outcomes to inputs are referred to as feed-forward, whereas networks that exhibit a looping synaptic link from outcomes to inputs are known as Recurrent Neural Networks (RNN). Neural network architectures are typically organized in layers. FFNNs can be classified as either single-layer or multi-layer networks, depending on the number of layers they contain. A completely linked, single-layer FFNN with two layers—with the exception of the input layer, which is devoid of any computations—is shown in Figure 2. Weights are used to transport signals from the input layers to the output layer, where neurons calculate the end result of the signals.

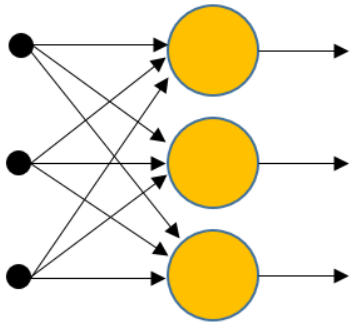

Figure 2. A feed-forward neural network with a single layer (Sarkar *et al*., 2020).

Figure 2 depicts a single-layer fully interconnected FFNN. With the input layer included, this framework consists of two levels. Therefore, since there are no computational processes performed in the input portion of the layer, it is not taken into account in the layer enumeration. The final outcome signals are computed by synapses in the signal generation layer after input signals are passed via weights to reach output (Sarkar *et al*., 2020).

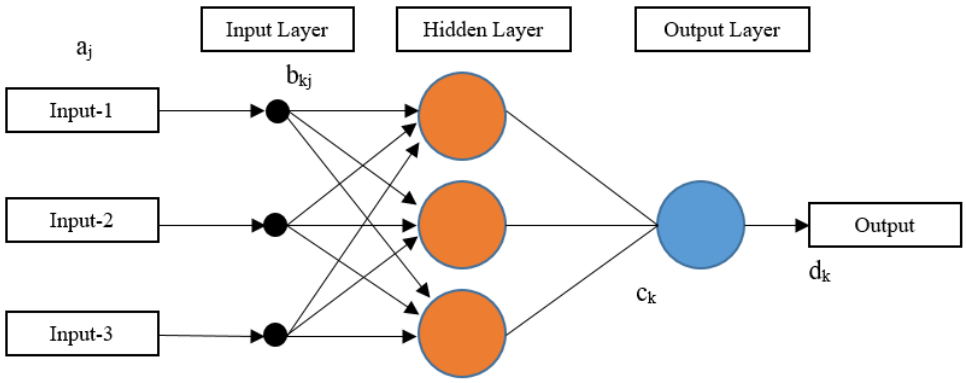

Figure 3. A feed-forward neural network with multiple layers (Sarkar *et al*., 2020).

Figure 3 demonstrates a FFNN with many layers and one hidden layer. The following architecture, corresponding to a single-layered network, includes a layer or number of hidden neurons that are positioned within the input layer and output layers, respectively. The characterization of a neuron *K* in scientific terms can be articulated using the subsequent Equations:

$$z_k = \sum_{j=1}^{n} b_{kj} a_j \tag{14}$$

$$d_k = \vartheta(z_k + c_k) \tag{15}$$

where, $a_1,a_2,a_3,.,a_n$ given the input signals initially; $b_{k1},b_{k2},b_{k3},..,b_{k3}$ are the strengthening connection of neurons *k*, commonly referred to as synaptic weights or simply weights; z_k represents the linear combination of input signals with their respective weights; c_k is termed as bias; the activation function is denoted by $\varphi(.)$; the final outcome of neuron is termed as d_k. Commonly employed activation functions include linear function, sigmoid, tan hyperbolic (tanh), among others. The role of the bias, a constant term is to modify the output z_k to ensure the optimal fit of the overall model for the provided data. The function that activates neurons evaluates the weights of synapses associated with each neuron and takes the bias into account when determining whether or not to stimulate a certain neuron.

The output of the neuron becomes nonlinear due to the mechanism of activation.These concealed neurons are meant to meaningfully intercede between the structure output and exterior feed. The network can retrieve higher-level statistics when it has more than one layers that are hidden. In the particular example shown in Figure 2, the system is classified as a 3-3-1 circuit since it has one hidden layer and three input neurons, three hidden neurons, and one output neuron. Figure 2 and Figure 3 shows the neural systems as fully interconnected, which indicates that each of the neurons in an individual layer has been linked to every other neuron in the layer of neurons that comes after it. Should any connections among neurons be missing, the neural network would be classified as described as partially connected.

2.3.2 Recurrent Neural Network (RNN)

Recurrent Neural Networks (RNNs) transcend the conventional feed-forward neural networks, elevated through the incorporation of recurrent edges that encapsulate contiguous temporal phases. This augmentation imparts a temporal dimension to the architectural design, introducing a nuanced concept of time within the network framework. While Recurrent Neural Networks (RNNs) are not obliged to exhibit explicit temporal phases within conventional boundaries, the integration of recurrent edges can dynamically give rise to distinct phases, encompassing auto links in the process. According to Musulin *et al*. (2021), the RNN is a member of the neural network class that handles sequential data processing. After receiving a

sequence of vectors ($x_1,x_2,..,x_n$) as input, they produce a second series ($h_1,h_2,..,h_n$) with information on the incoming sequence at each stage. RNNs manage variable-length classifications by operating a recurrent hidden state, where each initiation is influenced by the activation from the previous iteration.

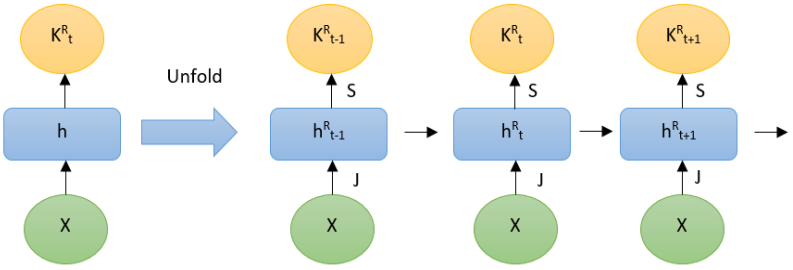

Figure 4. Structure of RNN model (Musulin *et al.*, 2020).

Figure 4 displays the RNN model architecture that how the updating of recurrent hidden state h^R_t is implemented as mentioned in Equation (16) and (17):

$$h_t^R = v\left(S.x_t + J.h_{t-1}^R + b\right) \tag{16}$$

$$K_t^R = v\left(S^0.h_t^R + b^0\right) \tag{17}$$

Here, *v* is a smooth, bounded function, such a logistic function or hyperbolic tangent and K^R_t is the result of a recurrent neural network, or its predicted value. The recurrent concealed state h^R_t at each time step t is determined by the input vector x_t, its preceding hidden state h^R_{t-1}. and the bias as b within the neural network architecture. The weight matrices, denoted as *S* and *J*, act as discerning filters, dictating the magnitude of significance attributed to the present input and the preceding hidden state. These matrices engender an error, subsequently harnessed in the process of backpropagation. This iterative feedback loop guides the adjustment of their parameters, iteratively refining the weights until further reduction of the error becomes unattainable (Faru *et al.*, 2023).

2.3.3 Formation of Hybrid Model

An efficient forecasting method by utilizing the advantages of a dual neural network approach, which effectively combines FFNN and RNN to estimate both Beta (the infection rate) and Delta (the death rate) parameters. The procedure starts with rigorous feature selection techniques from lasso regression, random forest and gradient boosting followed by the scaler standardization of the selected features dataset which is to be processed. The multi-layer FFNN is particularly good at identifying non-linear correlations in the features that it has chosen, while the RNN is very good at capturing the sequential connections that are present in the dataset. Through a concatenation layer, these separately optimized models are then smoothly combined into a single design, encouraging cooperation. The combined model is carefully trained on the provided dataset, supported by the beneficial FFNN-RNN synergy. The algorithm requirement for time-dependent coefficients suggests that time series predictions for the high accuracy coefficients are necessary.

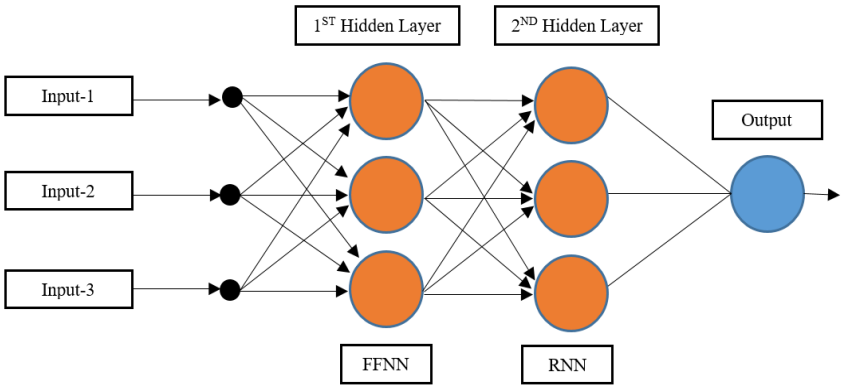

Figure 5. A Hybrid FNN-RNN architecture.

By utilizing the unique capabilities of the FFNN and RNN, the algorithms are strategically constructed as shown in Figure 5. Model coefficients can be forecasted by using historical data from the time frame {S(t),I(t),R(t),D(t),0<t<T-1}, where *t* denotes a particular day in the date range *T*. Analyzing the experimental data reveals that the simulator is capable of forecasting both beta (β) and delta (δ). The hybrid FFNN-RNN method provides inputs as β and δ to the SIRSD time-dependent model. When paired with feature selection approaches, the tactic based on deep learning yields estimated coefficients for the model beta(*t*) and delta(*t*), which serve as the primary prediction objectives. The efficacy of the model is evaluated and appreciated with the help of the training and validation loss. The aforementioned hybrid methodology provides a reliable and adaptable way to forecast infection and death rates based on the percentage set for the test dataset, as 30% in these experiments. It is enhanced by the thoughtful integration of feature selection techniques and the dynamic capabilities of FFNN-RNN that fulfills the objective of achieving higher accuracy.

2.4 The basic SIRD model

The SIR model is unique of the most extensively used and fundamental representations for predicting disease spread. It serves as the foundation for several variations, including the SIRD model (Bousquet *et al.*, 2022). The expansion of this infection is predicted, the total population afflicted, the length of the epidemic, and important epidemiological characteristics like the reproduction number are estimated, all with the help of the SIRD model. The mathematical model divisions individuals into four groups: susceptible, infected, recovered, and deceased. It also clarifies the changing patterns of virus-host connection throughout transmission. The death compartment is a new state that SIRD adds to the traditional SIR model. According to this framework, deaths are only ascribed to those who become infected (Bousquet *et al.*, 2022). Furthermore, *N* represents the overall population in the region at time t with $N = S(t)+I(t)+R(t)+D(t)$. The Equations (17-20) are expressed as:

$$\frac{dS}{dt} = -\frac{\beta IS}{N} \tag{17}$$

$$\frac{dI}{dt} = \frac{\beta IS}{N} - \gamma I - \mu I \tag{18}$$

$$\frac{dR}{dt} = \gamma I \tag{19}$$

$$\frac{dD}{dt} = \delta I \tag{20}$$

From this, β represents an infection rate, indicating the transition from susceptible to infected; The recovery rate, denoted by γ, represents the transition from infection to recovery, whereas the mortality rate, denoted by δ, represents the transfer from infection to death. The infection rate β,recovery rate γ and death rate δ, are the three parameters in the fundamental SIRD model that are considered to be fixed. This overlooks their time-dependent properties, which change continuously during the viral transmission process. In particular, we provide a time-dependent SIRSD framework, in which all four variables are defined as factors of time (t), to precisely and meritoriously predict the evolution of the infection. This approach offers a better treatment and enhanced capacity to predict future trend which is skilled at closely tracking the progression of the disease.

2.4.1 The time-varying SIRSD method

In order to fully understand the complexities of COVID-19 variability, re-infection scenarios must be included. As a consequence, the SIRD mechanism is extended to include a new compartment named Re-susceptible as 'RS' in the Equation (24), establishing the framework known as SIRSD. The obtained time-varying coefficients from hybrid approach as transmission rate (β) and mortality rate (δ) are fed into the SIRSD model along with the constant rate of recuperation (γ), and re-susceptible rate (α) as a concept of evolving variables that vary over time (t): $\beta(t)$,$\gamma(t)$,$\delta(t)$,$\alpha(t)$. We employed a numerical approximated performance to solve the SIRSD equations in order to construct the technique. We determine the fourth-order Runge–Kutta algorithm (RK4) for this research in order to integrate as time steps which results in the following discrete formulation of the SIRSD approach. The SIRSD+RK4 equation determined as:

$$\frac{dS(t)}{dt} = \frac{\beta(t)S(t)I(t)}{N} \tag{21}$$

$$\frac{dI(t)}{dt} = \frac{\beta(t)S(t)I(t)}{N} - \gamma(t)I(t) - \delta(t)I \tag{22}$$

$$\frac{dR(t)}{dt} = \gamma(t)I(t) \tag{23}$$

$$\frac{dRS(t)}{dt} = \alpha(t)R(t) \tag{24}$$

$$\frac{dD(t)}{dt} = \delta(t)I(t) \tag{25}$$

Throughout the COVID-19 spread, it is reasonable to assume a re-susceptible cases of approximately a thousand after every 20 days as individuals recovered and loses immunity towards the new emerging variants of disease. Assuming constant total population N the collective change in the state of each population whether an increase or decrease results in a net sum of 0.

$$\frac{dS(t)}{dt} + \frac{dI(t)}{dt} + \frac{dR(t)}{dt} + \frac{dRS(t)}{dt} + \frac{dD(t)}{dt} = 0 \tag{26}$$

To determine the Runge-Kutta method, we set as:

$$z = (SIRSD), H = equation(21-25), \tag{27}$$

Further, it follows:

$$\frac{dz}{dt} = H(t,z) \tag{28}$$

The Runge-Kutta method 4 can be expressed as:

$$z_{n+1} = z_n + \frac{f}{6}\left(q_1 + 2q_2 + 2q_3 + q_4\right) \tag{29}$$

$$q_1 = H\left(t_n, z_n\right) \tag{30}$$

$$q_2 = H\left(t_n + \frac{f}{2}, z_n + \frac{f\,q_1}{2}\right) \tag{31}$$

$$q_3 = H\left(t_n + \frac{f}{2}, z_n + \frac{f\,z_2}{2}\right) \tag{32}$$

$$q_4 = H\left(t_n + f, z_n + f\,q_3\right) \tag{33}$$

These equations describe the iterative process of updating the state vector q for each time step using the Runge-Kutta method. Here, H(t,z) represents the differential equations involved in the Runge-Kutta method, t_n is the current time, z_n is the current state, f is the step size, and z_{n+1} is the updated state. Through an iterative process involving the Runge-Kutta method, the model embeds the values of β and δ estimated by hybrid FFNN-RNN hybrid algorithm over time, taking into account the evolving nature of the pandemic. By comparing the predicted infected values with actual infected data, the Hybrid FFNN-RNN model offers a robust framework for forecasting and understanding the complexities of COVID-19 variability.

2.4.2 Performance Evaluation metrics

The algorithms predictive accuracy can be assessed by paralleling actual values with projected ones. To ensure a fair and comprehensive analysis, this study employs three evaluation metrics: mean absolute percentage error (MAPE), mean absolute error (MAE), and root mean square error (RMSE). Equations (34-36) describes how these measures are calculated:

$$MAPE = \frac{1}{N}\sum_{t=1}^{N}\left(\frac{\left|\hat{y}_i - y_i\right|}{y_i} * 100\%\right) \tag{34}$$

$$RMSE = \sqrt{\frac{1}{N}\sum_{i=1}^{N}(\hat{y}_i - y_i)^2} \tag{35}$$

$$MAE = \frac{1}{N}\sum_{i=1}^{N}\left|y_i - \hat{y}_i\right| \tag{36}$$

3. Results

Open-sourced libraries such as Numpy, Pandas, Tenserflow and Keras were used in the study presented in this article. High-level versatile programming language the Python is opted as it correlates well with artificial intelligence structures. Generating high-quality models is mostly dependent on the hyperparameters, which are the variables that describe the fundamental structure of the deep learning algorithm. For the simulation to work successfully, the hyperparameter measures must be determined. This study uses a customized tuning procedure to determine the best set of adapted hyperparameters, taking into account a variety of possible settings for each modified hyperparameter. Every possible pairing of hyperparameters is then defined and every possible combination of hyperparameters based upon selected features are then used for improving the deep learning algorithm. Each set of hyperparameters goes through multiple training rounds to reduce the likelihood of mistakes stemming from the early arbitrary weight values. The accuracy of each final model is then evaluated.

Table 4. Calibration of Hyperparameters Tuning.

Hyperparameter	Possible Calibration
Epochs	{10, 100, 1000}
Batch size	{32, 64}
Optimizer	{Adam}
Train and Test	70% and 30%
Feature Selection Techniques	Lasso Regression, Random Forest and Gradient Boosting

The chosen hyperparameters in Table 4 are best suited for optimizing the performance of the hybrid model and achieving desired results. We use historical Indian data for our experiment, which runs from the 15th of January 2021, to the 27th of May 2021. Epochs (10, 100, 1000) allow us to assess different training durations for balancing learning and overfitting. Batch sizes of 32 and 64 help evaluate the trade-off between training speed and model stability. The Adam optimizer is selected for its efficiency in adapting learning rates, facilitating faster convergence. A 70% train and 30% test split ensures sufficient data for robust training while allowing accurate performance evaluation. Finally, feature selection techniques like Lasso Regression, Random Forest, and Gradient Boosting help identify the most influential features, enhancing model accuracy and interpretability.

3.1 RQ1:Does the effectiveness and efficiency of the time-varying least-squares algorithm align with its underlying logic

The relevant dataset of India includes the susceptible individual cases, the contagion cases, the recovered cases and the death cases. We applied the least-squares method on multiple iterations to construct dataset to feed the obtained relevant coefficients such as infection rate (β) recovery rate (γ). These coefficients are critical in capturing the temporal variations in the spread of the virus and are used to validate the alignment of the algorithms effectiveness with its theoretical foundations. The iterative approach ensures that the model adapts to changes in real-time data, enhancing both the precision and reliability of the forecasts generated by the time-varying least-squares algorithm.

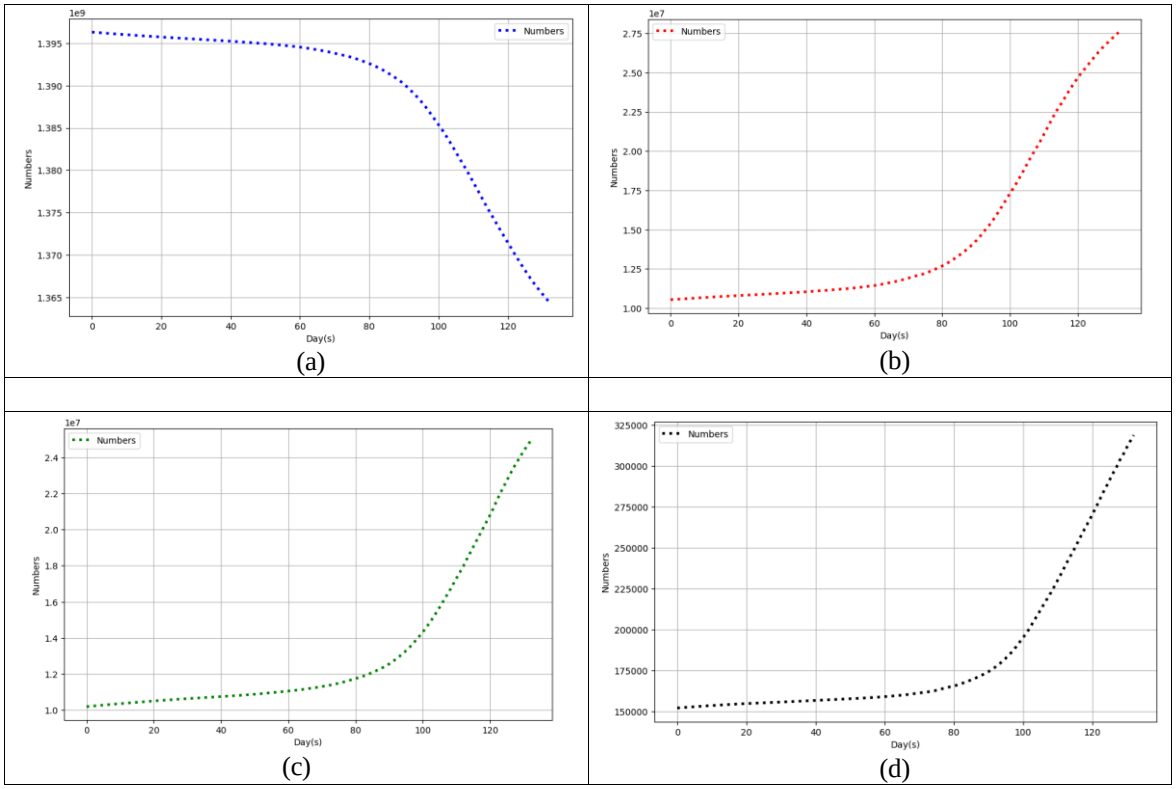

Figure 6. (a) Susceptible (b) Infected (c) Recovered and (d) Death for India dataset.

The susceptible, infected, recovered and death cases from 15th January, 2021, to 27th May, 2021 shown in Figure 6(a-d) to feed the machine learning for predicting required scenario coefficients with the support of feature selection techniques. It should be noted that the death rate (δ) is calculated separately after achieving the infection rate by integrating Equation (34):

$$\frac{dD(t)}{I(t)} = \delta(t) \tag{34}$$

Changes in genotype and cases of recurrent infections with different variations have been observed in COVID-19 recovered individuals following initial infection (Nguyen *et al*., 2023). In this context, the re-susceptibility rate (α) is assumed to be 1/20th of a day, while the recovery rate (γ) is set at 1/14th of a day (Nguyen *et al*., 2023). Analysis of the calculated parameters reveals that Day 90 marks the peak infection rate, indicating the highest increase in disease spread during the early phase of the outbreak. This finding validates the computations of the algorithm parameters. As illustrated in Figure 6(b), the recovery rate declines from Day 90 to Day 120, underscoring the critical need for timely interventions to manage case surges and prevent healthcare systems from being overwhelmed. The observed trends highlight the necessity of adaptive strategies in public health planning to mitigate the effects of future peaks in infection rates. Undertaking precise assumptions, such as the re-susceptibility and recovery rates, is essential for developing accurate predictive models. These assumptions allow for a clearer understanding of disease dynamics, which in turn informs effective public health responses and resource allocation. Accurate parameter estimation enables health authorities to anticipate potential surges in cases and plan accordingly, ensuring that healthcare resources are allocated efficiently. Furthermore, well-informed models can guide public communication strategies, helping to educate the public about the importance of vaccinations and other preventive measures. Ultimately, a solid foundation of precise assumptions enhances the credibility and utility of predictive models in combating infectious diseases.

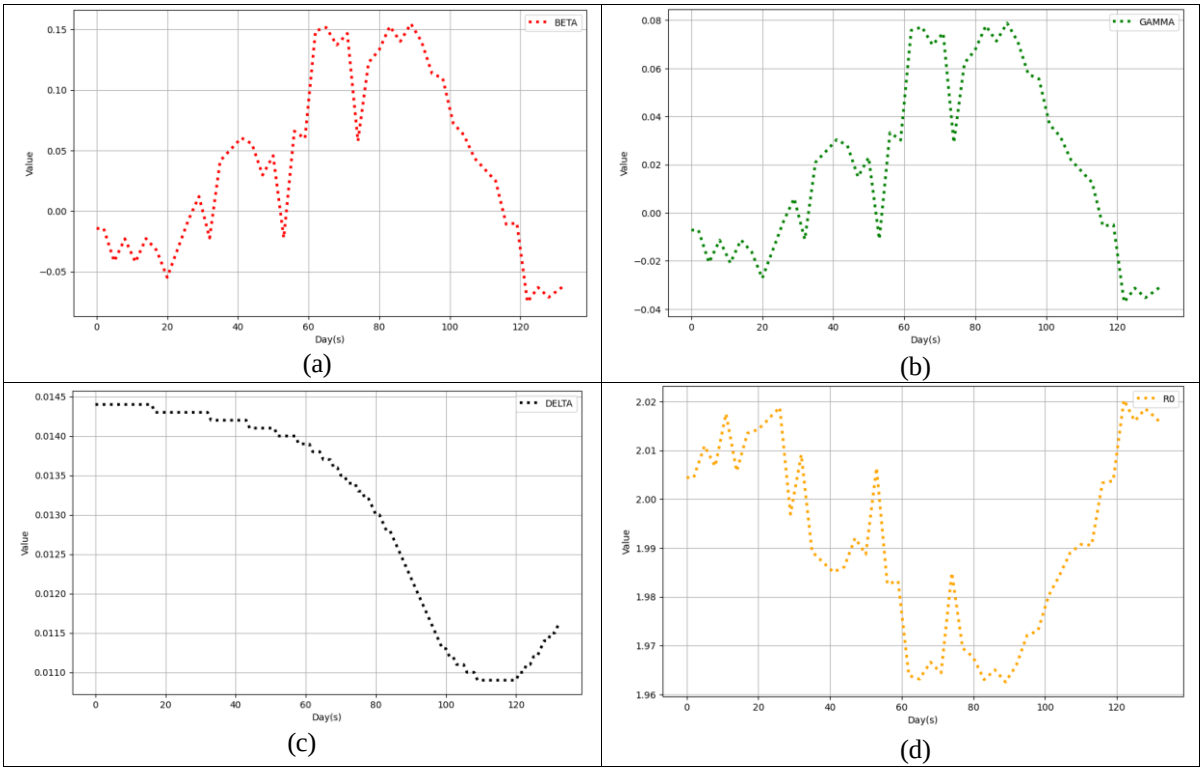

Figure 7. (a) Calculated rate of Infection β(t) (b) Calculated rate of Recovery γ(t) (c) Calculated rate of Death δ(t) and (d) Calculated rate of R_0(t).

The rate of mortality (δ) and R_0 in Figure 7(c-d) shows an increase after the infection spike, indicating a final peak in the overall amount of instances of reproduction and fatality. In general, the variables that were assessed by the use of the least squares approach function as a dependable gauge of variations in the epidemic actual time course. Interestingly, each measured simulation parameter shows periodic variations throughout time, as seen in Figure. 7(a-d), which lays the groundwork for future coefficient projections.

3.2 RQ2: What is the SIRSD-DL algorithm prediction achievement? How much better is it than standalone deep learning techniques? How about the algorithm efficacy for short- as well as intermediate duration predictions?

We performed a comparative study with Liao *et al.* (2021), who utilized deep learning techniques and mathematical models for predictions, to validate the efficiency of the proposed SIRSD-DL algorithm. The performance comparison focused on 1-day forecasting, comparing the SIRSD-DL approach with five additional forecasting models: GRU, Vanilla LSTM (the basic version of a Long Short-Term Memory network), Bi-Directional LSTM, Stacked LSTM, and SIRVD-DL. The experimental dataset used for this analysis comprised statistics from India, covering the period from April 18, 2021, to May 27, 2021. We conducted trials simultaneously for prediction spans of 1 day, 3 days, 7 days, 14 days, 21 days, and 28 days to evaluate the efficiency of the algorithm in both short- and medium-term projections. The SIRSD-DL produced a MAPE of 0.82% on first day, 1.65% on the third day, 3.10% on the seventh day, 3.50% on the fourteenth day, 2.92% on the twenty-first day, and 4.51% on the twenty-eighth day. The MAPE values, all less than 10%, indicate an improvement compared to the most advanced individual deep learning prediction techniques and mathematical models. The definitions of short- and medium-term can vary depending on the context and intended use; in this specific experiment, short-term predictions refer to horizons of 3 to 7 days, while medium-term predictions refer to horizons of 14, 21, and 28 days.

Table 5. 1-day forecasting outcomes of the test dataset comparison with the dataset employed by Liao *et al*., (2021)

Algorithms	RMSE	MAPE
Vanilla LSTM	151582.32	3.2921%
Stacked LSTM	92068.48	2.1498%
BiDirectional LSTM	145205.95	3.6597%
GRU	89787.23	1.8934%
SIRVD-DL	385128.55	0.92%
SIRSD-DL	127059.0	0.82%

Table 5 shows that SIRSD-DL outperforms other models in single-day forecasting across all evaluation metrics, achieving the lowest RMSE of 125,514.0 and 0.82 for MAPE value. The MAPE result shows that the proposed model continuously maintains a pretty high accuracy as the prediction time frame expands.

This implies that the models predictions achieve better accuracy in forecasting disease spread as the total number of calculated days increases. Considering all factors, the SIRSD-DL model demonstrates strong potential for making both short- and medium-term predictions. The training process completed efficiently in around 9 seconds, while testing was swift, yielding results in less than 1 second. Despite incorporating a hybrid deep learning framework, the model remains computationally efficient, as evidenced by its successful implementation on Google Colab using a modest mini laptop. This efficiency, combined with its high accuracy, makes it practical for real-world applications. The significance of these short and medium-term forecasts is critical for guiding public health strategies, helping administrations to determine control measures, manage compliance, and mitigate the strain on healthcare systems. Table 6 highlights the achieved discussed comparative results. Additionally, Figure 8 illustrates a contrast between the predicted and actual number of infections in India using the SIRSD-DL model.

Table 6. Comparing the predictive performance of SIRSD-DL and Liao's SIR prediction model (Liao *et al*., 2021)

Days	Metric	Bi-Directional LSTM	GRU	Stacked LSTM	Vanilla LSTM	SIRVD-DL	SIRSD-DL
3-day	MAPE %	5.51	5.48	6.23	4.58	2.51	1.48
7-day		8.92	12.4	18.3	6.5	5.07	2.72
14-day		31.71	46.2	98.22	24.09	10.93	2.50
21-day		53.01	62.05	85.82	34.88	17.89	3.73
28-day		89.29	79.21	85.95	86.53	26.57	6.63

Figure 8 contrasts the predicted numeral of infections with the actual numeral in India as estimated by the SIRSD-DL model.

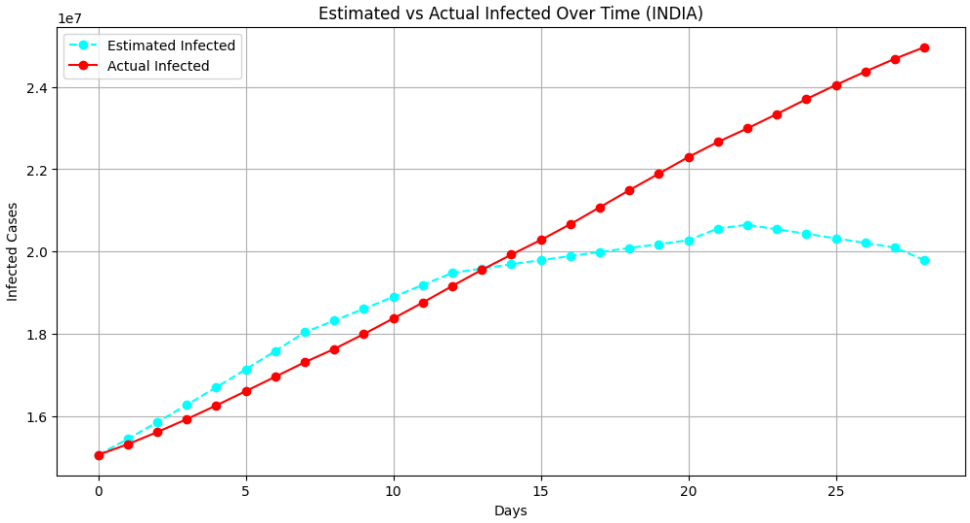

Figure 8. Comparison of Actual Infection cases versus Predicted Infection cases.

We used statistics from six diverse countries as China (Hubei), Malaysia, Pakistan, United States of America, United Arab Emirates and South Korea. This was done to test our approach and demonstrate the adaptability of our methodology. Each country had a different time frame for collecting COVID-19 data: China (March 11, 2020 – June 11, 2020), Malaysia (March 17, 2020 – June 17, 2020), Pakistan (March 18, 2020 – June 18, 2020), the United Arab Emirates (March 20, 2020 – June 20, 2020), the United States of America (March 5, 2020 – June 5, 2020), and South Korea (February 25, 2021 – May 27, 2021). The prediction results for these nations, obtained using the SIRSD-DL model, are shown in Table 7.

Table 7. Evaluating the performance of SIRSD-DL on selected nations datasets.

Country	Metric	1-day	3-day	7-day	9-day	11-day	14-day
China(Hubei)	MAPE %	1.12	2.05	3.36	3.92	4.83	9.18
Malaysia		0.59	0.82	1.74	2.46	3.18	4.06
Pakistan		1.77	2.74	2.32	2.20	2.63	4.42
South Korea		0.36	0.33	0.93	1.84	3.13	5.82
UAE		0.24	0.75	2.43	2.73	4.11	6.47
USA		0.43	1.06	2.32	2.57	2.84	2.99

3.3 RQ3: How well does the presented hybrid FFNN-RNN technique work for determining the coefficients when combined with feature selection? What distinguishes employing this procedure from not applying it?

To predict the infected cases, we initiated the procedure using three different feature selection techniques: LASSO, Random Forest, and Gradient Boosting. Next, we implemented scaler standardization to streamline the features onto a consistent scale, providing a baseline for input into our hybrid deep learning model. By analyzing the correlation among the selected features, as shown in Figures 9(a) and 9(b), these techniques indicated the most relevant features.

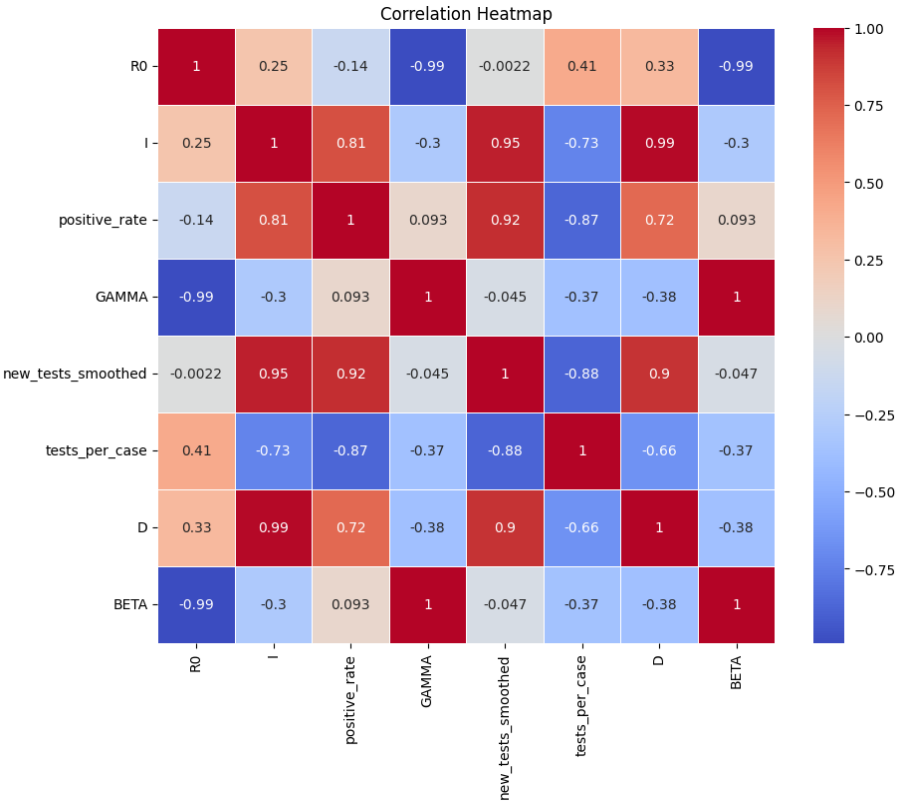

(a)

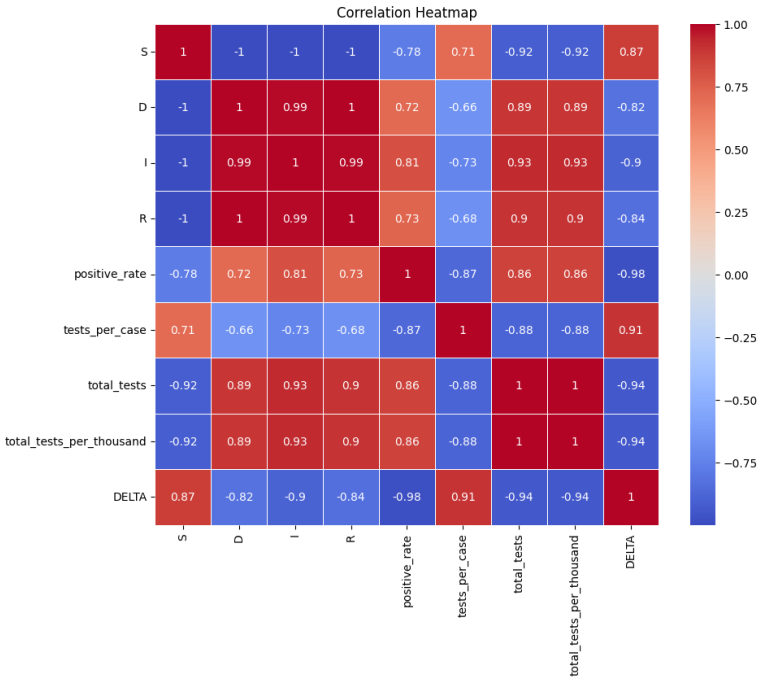

(b)

Figure 9. (a) Correlation for selecting features to estimate parameter β(t) and (b) Correlation for selecting features to estimate parameter δ(t).

These opted features periodically influences the algorithm parameters that are the rate of infection and rate of death during training process (70%) to make them more appropriate for time sequence prediction for test dataset (30%). Each neuron in the FFNN algorithm performs mathematical operations, such as functions of activation, skew addition, and weighted sums. Comparably, equations describing the recurrent step are used by the RNN to record sequential connections. The concatenation layer uses simple vector concatenation to

merge the results of the FFNN and RNN. Adam optimization which involves optimizing a loss function, updating weights, and computing gradients, is used in the course of training. The seamless design and implementation of this effective neural network architecture were made possible in large part by the TensorFlow neural network training framework. By implementation of this hybrid neural network approach, we achieved the best predicted parameters as shown in Figure 10(a-b) fulfilling the requirement to best fit the actual dataset and produce high efficiency prediction.

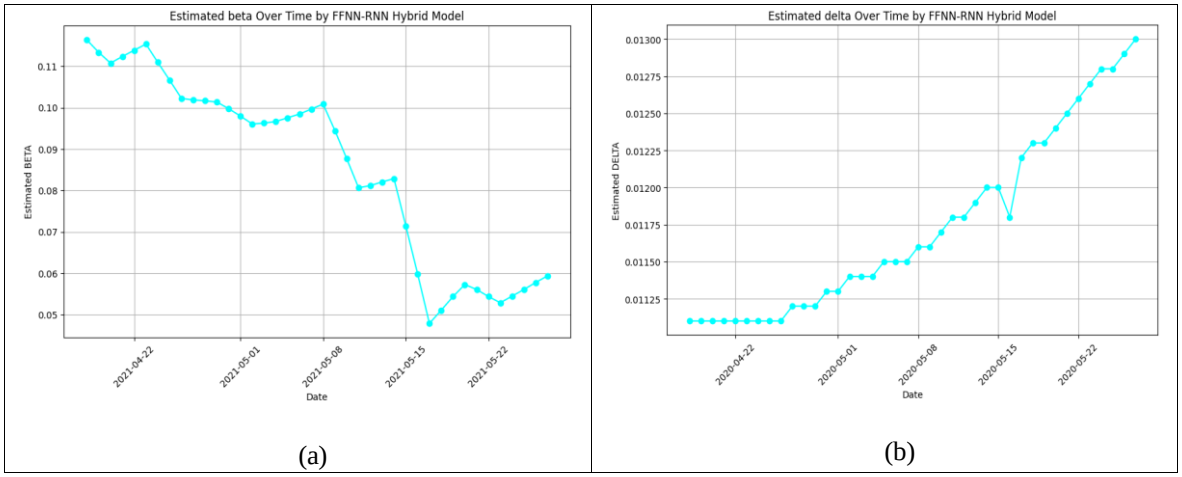

Figure 10. (a) A hybrid FFNN-RNN estimated parameters β(t) and (b) A hybrid FFNN-RNN estimated parameter δ(t).

We conducted comparative experiments by adjusting features to identify optimal parameters aligned with the epidemic trend aiming to enhance the precision of predicting the number of infected cases. Without feature selection, the algorithm would use all available features including potentially redundant ones. This can lead to a more complicated and inefficient hypothesis making it more difficult for it to pinpoint and isolate the key variables influencing infection rates. This would result in a less effective, adaptable, and focused. Poor accuracy in estimating infection numbers might result from the algorithms inability to discern significant patterns from the data particularly when dealing with dynamic and ever-changing settings.

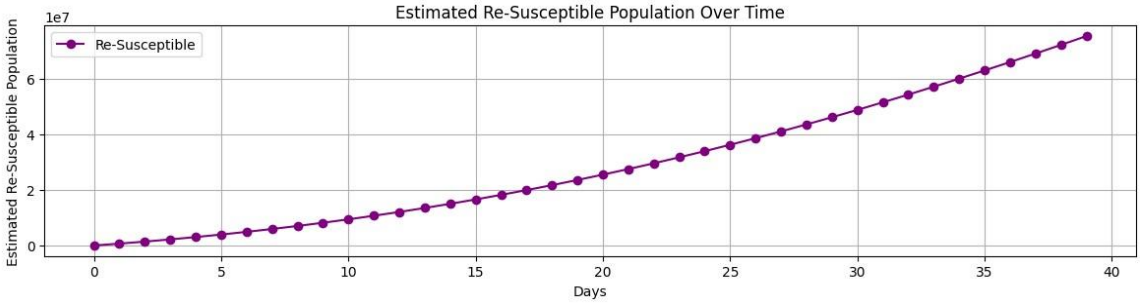

Figure 11. Analysis of Resusceptible cases α(t) (India).

The estimated re-susceptible population for India were also analyzed over a specified period as shown in Table 8. This analysis provides insight into the dynamics of re-susceptibility and its impact on the population over time. This trend underscores the focus on the dynamic nature of immunity against COVID-19 and its inferences for community health interventions. The increasing number of re-susceptible cases as shown in Figure 11 highlights the potential challenges in sustaining population-level immunity through natural infection, necessitating strategic controlling plans.

Table 8. Estimated Re-Susceptible cases (India).

Days	Estimated Re-susceptible	Percentage of total population
3-day	2,192,647	0.15%
7-day	5,939,191	0.42%
14-day	15,037,862	1.06%
21-day	27,681,607	1.95%
28-day	44,112,957	3.11%

By elucidating the gradual decline in immunity among recovered individuals, this analysis informs the imperative for ongoing surveillance and adaptive precautionary strategies to uphold resilience against future outbreaks. Such insights are pivotal in guiding policy makers and healthcare authorities in optimizing immunization efforts and mitigating the resurgence of these infections.

4. Conclusion

The COVID-19 pandemic has intensely obstructed daily life worldwide. On a global scale, extensive study has been led to comprehend the mechanisms of virus transmission, providing crucial information to governments and healthcare authorities. Numerous studies have proposed various COVID-19 forecasting methods, with particular attention to deep learning techniques, which are gaining significant interest within the scientific community. While deep learning algorithms can identify correlations in the temporal variations of infection rates and mathematical model demonstrated adequate prediction accuracy. To address the challenges in this domain, we introduced the SIRSD-DL approach, which forecasts key variables in viral infection simulations by integrating statistical epidemiological models with deep learning techniques. This integration enhances the interpretability and robustness of the overall projections, offering a significant advantage over traditional methods. Our experimental results indicate that the SIRSD-DL framework outperforms other approaches. Specifically, it improves single-day forecasts and shows strong performance in short- and medium-term projections with prediction errors of 0.82% for 1-day, 1.65% for 3-day, 3.10% for 7-day, 3.50% for 14-day, and 4.51% for 28-day forecasts, respectively. The robustness of SIRSD-DL is further validated by its consistent performance across various datasets from different countries, with an average MAPE of less than 10% over an 14-day period. This demonstrates the broad applicability of our algorithm for COVID-19 forecasting across diverse regions. Nevertheless, it is critical to concede the restrictions of our framework. One limitation lies in the accuracy of the datasets, as the statistics used are derived from publicly available sources, which may introduce discrepancies from real-world conditions. Additionally, the algorithm does not account for asymptomatic infections. Furthermore, this study does not incorporate vaccination rates or vaccine efficacy due to the challenges in data collection, which could lead to potential errors. Nonetheless, it is significant to recognize that these features could influence the predictive model. Looking ahead, there is significant potential for enhancing the SIRSD-DL model. Future iterations could incorporate vaccination rates, public health interventions, and other evolving factors such as emerging variants and behavioral changes. This flexibility would enable the model to adapt to future pandemics or infectious diseases, ensuring its relevance in dynamic public health scenarios. Incorporating such elements will not only improve prediction accuracy but also enhance the model's practical utility in aiding public health decision-making.

Data availability

Datasets can be downloaded from: https://github.com/owid/covid-19-data/tree/master/public/data/ and https://github. com/CSSEGISandData/COVID-19.

Acknowledgement

The authors would like to articulate our wholehearted appreciation to the Institute of Big Data Analytics and Artificial Intelligence (IBDAAI), Kompleks Al-Khawarizmi and Universiti Teknologi MARA (UiTM) for their high gratitude support and assistance.

Funding

The author(s) received no specific funding for this work.

Author Contribution

Author1 proposed the methodology and conceptualized the experiments and article writing. Author2 supervised the whole project and analyzed the statistical results. Author3 collected the datasets, selected the countries for experimentations and editing template. Author4 analyzed the manuscript and plotting the graphs. Author5 suggested the idea of utilizing least square method for calculating initial parameters and reviewed the manuscript and performed suitable editing according to the requirement of template.

Conflict of Interest

The authors have no conflicts of interest to declare.

References

Aimran, N., Rambli, A., Afthanorhan, A., Mahmud, A., Sapri, A., & Aireen, A. (2022). Prediction of Malaysian women divorce using machine learning techniques. Malaysian Journal of Computing, 7(2), 1067-1081. https://doi.org/10.24191/mjoc.v7i2.17077.

Anastassopoulou, C., Russo, L., Tsakris, A., & Siettos, C. (2020). Data-based analysis, modelling and forecasting of the COVID-19 outbreak. PLoS ONE, 15(3), e0230405. https://doi.org/10.1371/journal.pone.0230405.

Benardos, P. G., & Vosniakos, G. C. (2007). Optimizing feedforward artificial neural network architecture. *Engineering Applications of Artificial Intelligence*, 20(3), 365–382. https://doi.org/10.1016/j.engappai.2006.06.005.

Bousquet, A., Conrad, W. H., Sadat, S. O., Vardanyan, N., & Hong, Y. (2022). Deep learning forecasting using time-varying parameters of the SIRD model for Covid-19. *Scientific Reports*, 12(1). https://doi.org/10.1038/s41598-022-06992-0.

Chen, Y., Lu, P., Chang, C., & Liu, T. (2020). A Time-Dependent SIR model for COVID-19 with undetectable infected persons. *IEEE Transactions on Network Science and Engineering*, 7(4), 3279–3294. https://doi.org/10.1109/tnse.2020.3024723.

Chu, D., Singh, V., Ngoc, S. V., Nguyen, T., & Barceló, D. (2022). Transmission of SARS-CoV-2 infections and exposure in surfaces, points and wastewaters: A global one health perspective. *Case Studies in Chemical and Environmental Engineering*, 5, 100184. https://doi.org/10.1016/j.cscee.2022.100184.

Cooper, I., Mondal, A., & Antonopoulos, C. G. (2020). A SIR model assumption for the spread of COVID-19 in different communities. *Chaos Solitons & Fractals*, 139, 110057. https://doi.org/10.1016/j.chaos.2020.110057.

Devaraj, J., Elavarasan, R. M., Pugazhendhi, R., Shafiullah, G., Ganesan, S., Jeysree, A. K., Khan, I. A., & Hossain, E. (2021). Forecasting of COVID-19 cases using deep learning

models: Is it reliable and practically significant? *Results in Physics*, 21, 103817. https://doi.org/10.1016/j.rinp.2021.103817.

Faru, S. H., Waititu, A., & Nderu, L. (2023). A hybrid neural network model based on transfer learning for forecasting forex market. *Journal of Data Analysis and Information Processing*, 11(02), 103–120. https://doi.org/10.4236/jdaip.2023.112007.

Holmdahl, I., & Buckee, C. (2020). Wrong but useful — What COVID-19 epidemiologic models can and cannot tell us. *New England Journal of Medicine*, 383(4), 303–305. https://doi.org/10.1056/nejmp2016822.

Hu, B., Guo, H., Zhou, P., & Shi, Z. (2020). Characteristics of SARS-COV-2 and COVID-19. *Nature Reviews Microbiology*, 19(3), 141–154. https://doi.org/10.1038/s41579-020-00459-7.

Liao, Z., Lan, P., Fan, X., Kelly, B., Innes, A., & Liao, Z. (2021). SIRVD-DL: A COVID-19 deep learning prediction model based on time-dependent SIRVD. *Computers in Biology and Medicine*, 138, 104868. https://doi.org/10.1016/j.compbiomed.2021.104868.

Liao, Z., Lan, P., Liao, Z., Zhang, Y., & Liu, S. (2020). TW-SIR: time-window based SIR for COVID-19 forecasts. *Scientific Reports*, 10(1). https://doi.org/10.1038/s41598-020-80007-8.

Mohammadi, H., Rezapour, S., & Jajarmi, A. (2022). On the fractional SIRD mathematical model and control for the transmission of COVID-19: The first and the second waves of the disease in Iran and Japan. *ISA Transactions*, 124, 103–114. https://doi.org/10.1016/j.isatra.2021.04.012.

Musulin, J., Šegota, S. B., Štifanić, D., Lorencin, I., Anđelić, N., Šušteršič, T., Blagojević, A., Filipović, N., Ćabov, T., & Markova-Car, E. (2021). Application of Artificial Intelligence-Based Regression Methods in the Problem of COVID-19 Spread Prediction: A Systematic review. *International Journal of Environmental Research and Public Health*, 18(8), 4287. https://doi.org/10.3390/ijerph18084287.

Nabi, K. N., Tahmid, T., Rafi, A., Kader, M. E., & Haider, M. A. (2021). Forecasting COVID-19 cases: A comparative analysis between recurrent and convolutional neural networks. *Results in Physics*, 24, 104137. https://doi.org/10.1016/j.rinp.2021.104137.

Nguyen, N. N., Nguyen, Y. N., Hoang, V. T., Million, M., & Gautret, P. (2023). SARS-COV-2 Reinfection and Severity of the Disease: A Systematic Review and Meta-Analysis. *Viruses*, 15(4), 967. https://doi.org/10.3390/v15040967.

Panovska-Griffiths, J. (2020). Can mathematical modelling solve the current Covid-19 crisis? *BMC Public Health*, 20(1). https://doi.org/10.1186/s12889-020-08671-z.

Ramezani, S. B., Amirlatifi, A., & Rahimi, S. (2021). A novel compartmental model to capture the nonlinear trend of COVID-19. *Computers in Biology and Medicine*, 134, 104421. https://doi.org/10.1016/j.compbiomed.2021.104421.

Rudin, C. (2019). Stop explaining black box machine learning models for high stakes decisions and use interpretable models instead. *Nature Machine Intelligence*, 1(5), 206–215. https://doi.org/10.1038/s42256-019-0048-x.

Sarkar, P. P., Janardhan, P., & Roy, P. (2020). Prediction of sea surface temperatures using deep learning neural networks. *SN Applied Sciences*, 2(8). https://doi.org/10.1007/s42452-020-03239-3.

Singh, P., & Gupta, A. (2022). Generalized SIR (GSIR) epidemic model: An improved framework for the predictive monitoring of COVID-19 pandemic. *ISA Transactions*, 124, 31–40. https://doi.org/10.1016/j.isatra.2021.02.016.

Tang, L., Zhou, Y., Wang, L., Purkayastha, S., Zhang, L., He, J., Wang, F., & Song, P. X. (2020). A review of Multi-Compartment infectious disease models. *International Statistical Review*, 88(2), 462–513. https://doi.org/10.1111/insr.12402.

Van Doremalen, N., Bushmaker, T., Morris, D. H., Holbrook, M. G., Gamble, A., Williamson, B. N., Tamin, A., Harcourt, J. L., Thornburg, N. J., Gerber, S. I., Lloyd-Smith, J. O., De Wit, E., & Munster, V. J. (2020). Aerosol and Surface Stability of SARS-CoV-2 as Compared with SARS-CoV-1. *New England Journal of Medicine*, 382(16), 1564–1567. https://doi.org/10.1056/nejmc2004973.

Zeroual, A., Harrou, F., Dairi, A., & Sun, Y. (2020). Deep learning methods for forecasting COVID-19 time-Series data: A Comparative study. *Chaos Solitons & Fractals*, 140, 110121. https://doi.org/10.1016/j.chaos.2020.110121.

Zhang, P., Feng, K., Gong, Y., Lee, J., Lomonaco, S., & Zhao, L. (2022). Usage of compartmental models in predicting COVID-19 outbreaks. *The AAPS Journal*, 24(5). https://doi.org/10.1208/s12248-022-00743-9